ISBN: 978-3-95450-184-7 doi:10.18429/JACoW-IPAC2018-TUPAF030

ELECTRON CLOUD BUILD UP FOR LHC 'SAWTOOTH' VACUUM CHAMBER*

G. Guillermo †, Cinvestav del IPN, Mérida, México, and CERN, Geneva, Switzerland
G.H.I. Maury Cuna, E.D. Ocampo Ortiz, Departamento de Física,
Universidad de Guanajuato, León, México
F. Zimmermannn, CERN, Geneva, Switzerland

Abstract

At high proton-beam energies, beam-induced synchrotron radiation is an important source of heating, of beam-related vacuum pressure increase, and of primary photoelectrons, which can give rise to an electron cloud. For the arcs of LHC a sawtooth pattern had been imprinted on the horizontally outward side of the vacuum chamber in order to locally absorb synchrotron radiation photons without dispersing them all around the chamber. Using the combination of the codes Synrad3D and PyECLOUD, we examine the effect of realistic absorption distributions with and without sawtooth on the build up of electron clouds.

INTRODUCTION

In the arcs of the LHC a sawtooth pattern is imprinted on the horizontally outward side of the so-called beam screen, in order to locally absorb beam-induced synchrotron radiation and to avoid dispersing it towards the top and bottom of the dipole-magnet vacuum chamber, where it could become seeds for an electron cloud. In previous work [1–4] we have attempted to iteratively obtain a more and more realistic photon distribution function (PDF), by which we mean the azimuthal distribution of absorbed photons in the vacuum chamber of the LHC arcs. PDFs were obtained by means of the photon tracking code Synrad3D [5]. In a first step [1] we used the LHC vacuum chamber shape, but neglected the sawtooth pattern, which is imprinted on the outer side of the wall. In a second step [2] we included an ideal model of this sawtooth pattern. In a recent third step [6] we have improved the model by adjusting certain parameters, according to measurements performed on an actual beam-pipe sample at BESSY II. We here present results from electron-cloud build-up simulations, considering PDFs computed by Synrad3D for the distribution of primary photoelectrons.

MOTIVATION

After the LHC incident in 2008, a number of LHC arc dipole beam screens were installed with an inverted sawtooth pattern (a situation which we will refer to as "inverted sawtooth") [7]. Figure 3 shows the model of the LHC inverted sawtooth beam screen as implemented in the code Synrad3D.

* This work was supported, in part, by the European Commission under the HORIZON 2020 Integrating Activity project ARIES, Grant Agreement No. 730871, and by the Mexican CONACyT "BEAM" Program.
† Gerardo.Guillermo.Canton@cern.ch

Table 1: PyECLOUD Main Simulation Parameters

arameter	alue
Secondary emission yield	1.0–1.7
beam energy	7 TeV
bunch spacing	25 ns

PHOTON DISTRIBUTION FUNCTIONS

Using the code Synrad3D [5], we tracked photons in the LHC arcs from emission to absorption through any number of intermediate reflections. Our vacuum-chamber model is shown in Fig. 1. The chamber material was treated as a 10 nm carbon layer on a copper substrate with a surface roughness (σ) of 50 nm, based on laboratory measurements of a conditioned chamber; further improvements to the model are presented in [6]; others are planned. The underlying optics lattice file is HL-LHC version 1.1 (presqueeze) [8], which in the arcs equals the optics of LHC, at top energy, i.e. 7 TeV. The PDF was obtained for three cases: a) a "smooth chamber", without any sawtooth pattern; b) a regular "sawtooth"; and c) an inverted sawtooth, where the sawtooth was placed with inverted orientation (as shown in Fig. 1c)). In Fig. 2 the normalized azimuthal distribution of absorbed photons is shown for the aforementioned three cases.

PyECLOUD

PyECLOUD is a 2D macro-particle code capable of simulating an electron cloud (EC) build-up in particle accelerators like the LHC [9]. For the present studies, we uses a modified branch of the code version 6.6.0, provided by G. Iadarola, which permits the code to launch photoelectrons from a distribution defined by a separate input file. Thanks to this modification we were able to feed PyECLOUD with the PDFs generated by Synrad3D. For the EC simulations we used the parameters reported in Table 1. We considered a nominal LHC filling pattern consisting of 4 trains of 72 bunches and a train spacing of 225 ns. We carried out three sets of simulations, each for a different PDF, corresponding to the three beam-pipe surface configurations introduced above, namely 1) without sawtooth pattern (smooth), 2) sawtooth pattern with correct orientation and 3) an inverted orientation for the sawtooth pattern.

RESULTS

In Figure 3, we show a typical EC build-up behavior for the three different vacuum-chamber surfaces considered. The

ISBN: 978-3-95450-184-7 doi:10.18429/JACoW-IPAC2018-TUPAF030

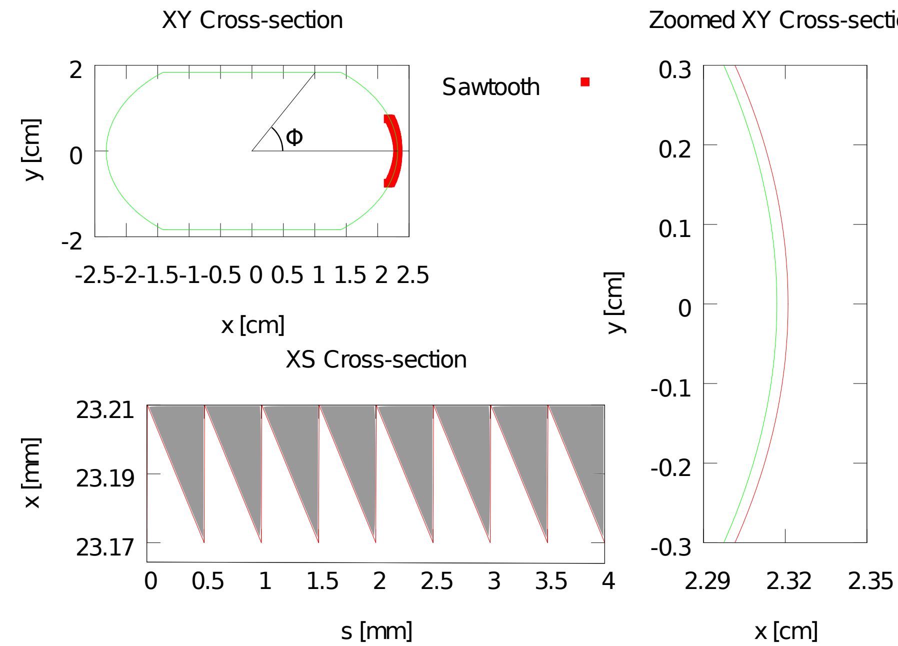

Figure 1: Synrad3D model of the LHC beam-screen design. (a) xy beam-screen cross section, (b) enlarged view of the sawtooth portion of the xy cross section, (c) xs cross section. A beam moving towards the positive s direction will see an inverted sawtooth; a beam moving towards negative s will witness the correct form of the sawtooth. [4]

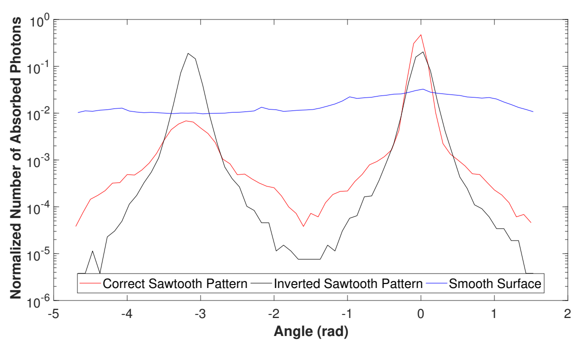

Figure 2: Simulated azimuthal distribution (integral normalized to unity) of absorbed photons without (blue curve) and with a sawtooth (red curve) and with an inverted sawtooth (black curve) chamber. [4]

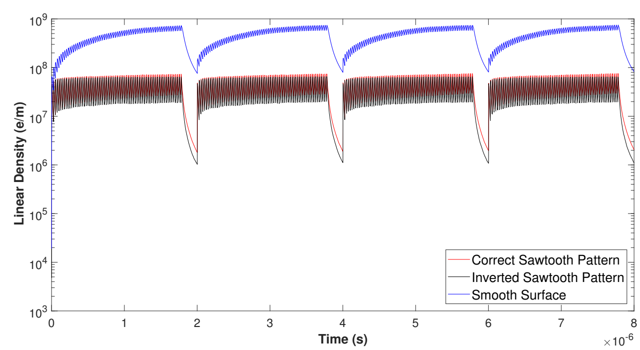

Figure 3: Electron linear density for a SEY = 1.3 and for a smooth chamber (blue curve), a sawtooth pattern correctly oriented (red curve) and an inverted-orientation sawtooth pattern (black curve).

case for a secondary emission yield (SEY) of 1.3 is depicted as an example, comparing the three vacuum chamber surface configurations. The EC linear density evolves as a function of time as the four trains are passing through an LHC arc dipole section.

Linear Electron Density

In Figure 4 we present the average linear electron density as a function of the SEY. The average has been taken over the entire simulation time. We notice that the linear density is higher for a chamber with a smooth surface, and lower for the surfaces with the pattern imprinted on them. For all values of SEY, the lowest electron density is obtained with the sawtooth of inverted orientation.

Electron-Cloud Heat Load

Figure 5 shows the average heat load per unit length as a function of the SEY for each of the three surface configurations. The smooth surface chamber exhibits the highest values of heat load. Similar to the finding for the linear density, the inverted sawtooth yields a (slightly) smaller heat load than the correctly oriented sawtooth.

DISCUSSION

We observe a significant effect of the different surface configurations on the simulated electron line density and heat load, as shown in Figs. 4 and 5, respectively. At top energy, for SEY values between 1.0 to 1.3 the linear density increases by a factor of 3 to 8; at SEY values above

ISBN: 978-3-95450-184-7 doi:10.18429/JACoW-IPAC2018-TUPAF030

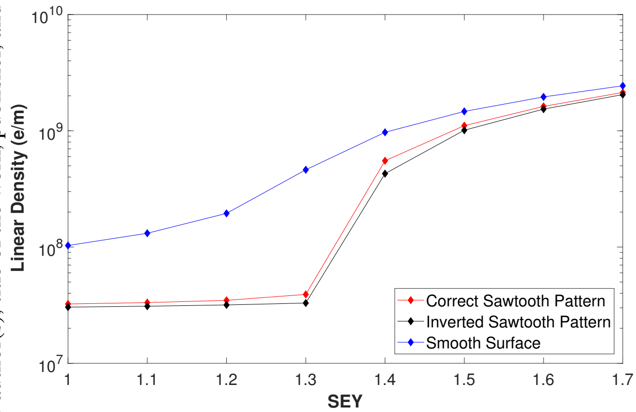

Figure 4: Average linear density as a function of SEY for three vacuum surfaces: smooth chamber (blue curve), correctly oriented sawtooth (red curve), and inverted sawtooth (black curve).

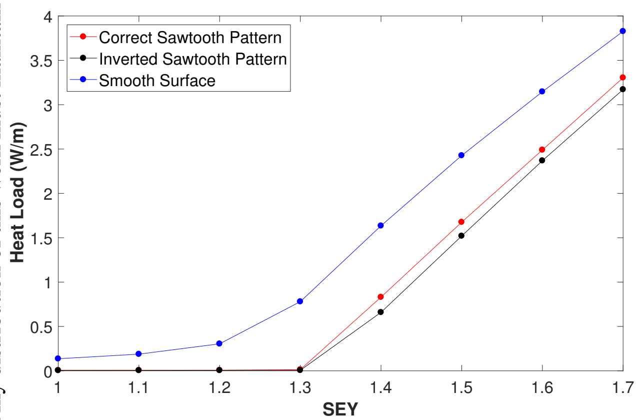

Figure 5: Average heat load as a function of secondary emission yield (SEY) for three vacuum surfaces: smooth chamber (blue curve), correctly oriented sawtooth (red curve) and sawtooth with inverted orientation (black curve).

1.4, where the build up approaches saturation, the sawtooth pattern becomes comparatively less effective. The inverted sawtooth pattern is the configuration that gives rise to the lowest electron linear density and heat load by a tiny amount. It, therefore, seems that the inverted sawtooth is slightly more effective that the correct sawtooth, however, the PDF is highly dependent on the surface roughness of the material and our PDFs are valid for very low surface roughness (σ) of order 50 nm, which is the value expected for the LHC chamber; and the current model does not include imperfections.

Future Work

The presented results are based on a standard LHC beam filling pattern. Further work will consider the LHC filling pattern of 2017, and also scan a large range of surface roughnesses (σ values). In addition, the effect of the PDF on EC build up in LHC beamline components other than dipole magnets will be studied, e.g. in quadrupoles and no-field regions. Other ongoing work is directed towards improving the vacuum chamber model and to validating the simulated PDFs, by closing the gap between experimental measurements and simulations [6]

ACKNOWLEDGEMENTS

We would like to thank M. Giovannozzi, G. Iadarola, and E. Métral at CERN, and L. Mether at EPFL for several helpful discussions. These simulations would not have been possible without the strong support from D. Sagan at Cornell University. G. Guillermo is grateful to TRIUMF ("centre canadien d'accélération des particules") for an IPAC'18 student grant, and to the Secretaría de Educación Pública for the support within the frame of the project "Apoyo a la incorporación de NPTC de PRODEP" with number SEP UGTO-PTC-607. Travel to IPAC'18 supported by the United States National Science Foundation, the Division of Physics of Beams of the American Physical Society, and TRIUMF.

REFERENCES

[1] G. Maury *et al.*, "Synchrotron-radiation photon distribution for highest energy circular colliders," in *Proc. 4th International Particle Accelerator Conferenc*, p. 1340, May 2013.

[2] G. Guillermo, D. Sagan, and F. Zimmermann, "Simulating Proton Synchrotron Radiation in the Arcs of the LHC, HL-LHC and FCC-hh," in *Proc. of Int. Particle Accelerator Conf.*, pp. 2073–2076, JACoW, June 2016.

[3] G. Guillermo Canton, M. Ady, M. Angelucci, R. Cimino, R. Kersevan, E. La Francesca, D. Sagan, and F. Zimmermann, "Comparing Behaviour of Simulated Proton Synchrotron Radiation in the Arcs of the LHC with Measurements," in *Proceedings, 8th International Particle Accelerator Conference (IPAC 2017): Copenhagen, Denmark, May 14-19, 2017*, 2017.

[4] G. Guillermo, D. Sagan, and F. Zimmermann, "Examining mitigation schemes for synchrotron radiation in high-energy hadron colliders," *Phys. Rev. Accel. Beams*, vol. 21, p. 021001, Feb 2018.

[5] G. Dugan and D. Sagan, "Simulating synchrotron radiation in accelerators including diffuse and specular reflections," *Phys. Rev. Accel. Beams*, vol. 20, p. 020708, Feb 2017.

[6] G. Guillermo Canton, M. Angelucci, R. Cimino, I. Bellafont, A. Liedl, E. La Francesca, D. Sagan, and F. Zimmermann, "Improved Benchmarking of Laboratory reflectivity Data and Simulations for a Sawtooth Chamber," in *Proceedings, 9th International Particle Accelerator Conference (IPAC 2018): Vancouver, Canada, April 29- May 4, 2018*, 2018.

[7] N. Kos, *Change of beam screen types in Cryo-dipoles for sector 3-4*. LHC-VSS-EC-0010 ver. 1.0, EDMS Document no. 98531, Geneva: CERN, 2004. https://edms.cern.ch/document/985318/1.0.

[8] R. de Maria, "HL-LHC version 1.1 'Presqueeze optics'," viewed 11 May 2017. http://abpdata.web.cern.ch/abpdata/lhc_optics_web/www/hllhc11/.

[9] G. Iadarola, E. Belli, K. Li, L. Mether, A. Romano, and G. Rumolo, "Evolution of Python Tools for the Simulation of Electron Cloud Effects," no. CERN-ACC-2017-240, 2017. http://cds.cern.ch/record/2289165.